AIMS Mathematics, 8(6): 13205–13218.
DOI:10.3934/math.2023667
Received: 08 December 2022
Revised: 06 March 2023
Accepted: 20 March 2023
Published: 03 April 2023

http://www.aimspress.com/journal/Math

Research article

Numerical simulation of fractional-order two-dimensional Helmholtz equations

Naveed Iqbal[1,*], Muhammad Tajammal Chughtai[2] and Nehad Ali Shah[3]

[1] Department of Mathematics, College of Science, University of Ha'il, Ha'il 2440, Saudi Arabia
[2] Department of Electrical Engineering, College of Engineering, University of Ha'il, Ha'il 55427, Saudi Arabia
[3] Department of Mechanical Engineering, Sejong University, Seoul 05006, Korea

* **Correspondence:** Email: n.iqbal@uoh.edu.sa.

Abstract: In this paper, we investigate the exact solutions of several fractional-order Helmholtz equations using the homotopy perturbation transform method. We specify sufficient requirements for its convergence and provide error estimations. The homotopy perturbation transform method yields a quickly converging succession of solutions. Solutions for various fractional space derivatives are compared to present approaches and explained using figures. Appropriate parameter selection produces approximations identical to the exact answer. Test examples are provided to demonstrate the proposed approach's precision and competence. The results demonstrate that our system is appealing, user-friendly, dependable, and highly effective.

Keywords: fractional Helmholtz equations; Caputo operator; homotopy perturbation transform method; analytical solution
Mathematics Subject Classification: 33B15, 34A34, 35A20, 35A22, 44A10

1. Introduction

In recent years, fractional differential equations have gained prominence due to their proven usefulness in several unrelated scientific and engineering fields. For example, the nonlinear oscillations of an earthquake can be characterized by a fractional derivative, and the fractional derivative of the traffic fluid dynamics model can solve the insufficiency resulting from the assumption of continuous traffic flows [1–3]. Numerous chemical processes, mathematical biology, engineering, and scientific problems [4–7] are also modeled with fractional differential equations. Nonlinear partial differential equations (NPDEs) characterize various physical, biological, and chemical phenomena. Current research is focused on developing precise traveling wave solutions for such equations. Exact

and explicit solutions help scientists understand the complicated physical phenomena and dynamic processes portrayed by NPDEs [8–10]. In the past four decades, numerous essential methodologies for attaining accurate solutions to NPDEs have been proposed [11, 12].

The Helmholtz equation (HE) derives from the elliptic and wave equations. In a multi-dimensional nonhomogeneous isotropic standard with velocity c, the wave result is $\upsilon(\xi, \psi)$, which corresponds to a source of harmonic (ξ, ψ) vibrating at a given frequency and satisfying the Helmholtz equation in the area R. The classical order HE is

$$D_{\xi}^{2}\upsilon(\xi, \psi) + D_{\psi}^{2}\upsilon(\xi, \psi) + \varepsilon\upsilon(\xi, \psi) = -\upsilon(\xi, \psi). \tag{1.1}$$

Here, υ is a suitable boundary differentiable term of R, is a known function, and the wave number with wavelength $2/\xi = 0$ renders Eq (1.1) homogeneous. If (1.1) is expressed as

$$D_{\xi}^{2}\upsilon(\xi, \psi) + D_{\psi}^{2}\upsilon(\xi, \psi) - \varepsilon\upsilon(\xi, \psi) = -\upsilon(\xi, \psi).$$

Then it explains mass transfer with density biochemical processes of the 1st order. Equation (1.1) is investigated using the decomposition method [13], the finite element approach [14], the differential transform method [15], the Trefftz method [16], and the spectral collocation method [17], among others [18–20].

The Helmholtz equation is a partial differential equation that describes wave phenomena in various fields of physics, such as electromagnetism, acoustics, and fluid mechanics. Traditionally, the Helmholtz equation has been formulated using integer-order derivatives. However, in recent years, there has been a growing interest in the use of fractional-order derivatives to describe complex phenomena more accurately. In particular, fractional-order space Helmholtz equations are derived directly from mathematical formulas that involve fractional derivatives, rather than being generalized from integer-order space derivative Helmholtz equations. These equations can provide a more accurate description of wave propagation in complex media, such as porous materials, biological tissues, and fractal structures. Fractional-order space Helmholtz equations have attracted significant attention due to their potential applications in a wide range of fields, including medical imaging, geophysics, and telecommunications. They offer a promising avenue for understanding the behavior of waves in complex media and developing new technologies for wave-based sensing and imaging [21–23].

It is advantageous to utilize fractional differential equations in physical problems due to their nonlocal features. Non-locality characterizes fractional-order derivatives, whereas locality characterizes integer-order derivatives [24–27]. It demonstrates that the future state of the physical system depends on all of its previous states in addition to its current state. Consequently, fractional models are more accurate. In fractional differential equations, the response expression has a parameter that specifies the fractional derivative of the variable order, which may vary to achieve many responses [28–30].

Standard HEs can be generalized to fractional-order Helmholtz equations by extending the Caputo fractional-order space derivative to the integer-order space derivative. The fractional Helmholtz equation in space is

$$D_{\xi}^{\varrho}\upsilon(\xi, \psi) + D_{\psi}^{2}\upsilon(\xi, \psi) + \varepsilon\upsilon(\xi, \psi) = -\psi(\xi, \psi),$$

with $\upsilon(0, \psi) = g(\psi)$ as the initial condition (IC). Gupta et al. [31] solved the multi-dimensional fractional Helmholtz equation using the homotopy perturbation approach. In contrast, Abuasad

et al. [14] recently solved a fractional model of the Helmholtz problem using the reduced differential transform method.

2. Preliminary concepts

This section describes the properties of the fractional derivatives and a few essential details concerning the Yang transform.

Definition 2.1. *The fractional derivative in terms of Caputo is as follows*

$$D_{\psi}^{\varrho}\upsilon(\xi,\psi)=\frac{1}{\Gamma(k-\varrho)}\int_{0}^{\psi}(\psi-\varrho)^{k-\varrho-1}\upsilon^{(k)}(\xi,\varrho)d\varrho,\quad k-1<\varrho\leq k,\quad k\in N. \tag{2.1}$$

Definition 2.2. *The YT is represented as follows*

$$Y\{\upsilon(\psi)\}=M(u)=\int_{0}^{\infty}e^{\frac{-\psi}{u}}\upsilon(\psi)d\psi,\ \ \psi>0,\ \ u\in(-\psi_1,\psi_2), \tag{2.2}$$

having inverse YT as follows

$$Y^{-1}\{M(u)\}=\upsilon(\psi). \tag{2.3}$$

Definition 2.3. *The nth derivative YT is stated as follows*

$$Y\{\upsilon^{n}(\psi)\}=\frac{M(u)}{u^{n}}-\sum_{k=0}^{n-1}\frac{\upsilon^{k}(0)}{u^{n-k-1}},\ \ \forall\ \ n=1,2,3,\cdots \tag{2.4}$$

Definition 2.4. *The YT of derivative having fractional-order is stated as follows*

$$Y\{\upsilon^{\varrho}(\psi)\}=\frac{M(u)}{u^{\varrho}}-\sum_{k=0}^{n-1}\frac{\upsilon^{k}(0)}{u^{\varrho-(k+1)}},\ \ 0<\varrho\leq n. \tag{2.5}$$

3. General implementation of the method

Consider the general fractional partial differential equations,

$$\begin{aligned}&D_{\psi}^{\varrho}\upsilon(\xi,\psi)+M\upsilon(\xi,\psi)+N\upsilon(\xi,\psi)=h(\xi,\psi),\quad \psi>0,\quad 0<\varrho\leq 1,\\&\upsilon(\xi,0)=g(\xi),\quad \nu\in\Re.\end{aligned} \tag{3.1}$$

Using Yang transform of Eq (3.1), we get

$$\begin{aligned}&Y[D_{\psi}^{\varrho}\upsilon(\xi,\psi)+M\upsilon(\xi,\psi)+N\upsilon(\xi,\psi)]=Y[h(\xi,\psi)],\quad \psi>0,0<\varrho\leq 1,\\&\upsilon(\xi,\psi)=sg(\xi)+s^{\varrho}Y[h(\xi,\psi)]-s^{\varrho}Y[M\upsilon(\xi,\psi)+N\upsilon(\xi,\psi)].\end{aligned} \tag{3.2}$$

Now, applying inverse Yang transform, we have

$$\upsilon(\xi,\psi)=F(\xi,\psi)-Y^{-1}\left[s^{\varrho}Y\{M\upsilon(\xi,\psi)+N\upsilon(\xi,\psi)\}\right], \tag{3.3}$$

where

$$F(\xi,\psi) = Y^{-1}\left[sg(\xi) + s^{\varrho}Y[h(\xi,\psi)]\right] = g(\nu) + Y^{-1}\left[s^{\varrho}Y[h(\xi,\psi)]\right]. \tag{3.4}$$

The parameter p is perturbation technique and $p \in [0,1]$ defined as

$$\upsilon(\xi,\psi) = \sum_{k=0}^{\infty} p^k \upsilon_k(\xi,\psi), \tag{3.5}$$

The nonlinear function is expressed as

$$N\upsilon(\xi,\psi) = \sum_{k=0}^{\infty} p^k H_k(\upsilon_k), \tag{3.6}$$

where H_n are He's polynomials in term of $\upsilon_0, \upsilon_1, \upsilon_2, \cdots, \upsilon_n$, and can be calculated as

$$H_n(\upsilon_0, \upsilon_1, \cdots, \upsilon_n) = \frac{1}{\varrho(n+1)} D_p^{\iota}\left[N\left(\sum_{\iota=0}^{\infty} p^{\iota}\upsilon_{\iota}\right)\right]_{p=0}, \tag{3.7}$$

where $D_p^{\iota} = \frac{\partial^{\iota}}{\partial p^{\iota}}$.

Putting Eqs (3.6) and (3.7) in Eq (3.3), we achieved as

$$\sum_{\iota=0}^{\infty} p^{\iota}\upsilon_{\iota}(\xi,\psi) = F(\xi,\psi) - p \times \left[Y^{-1}\left\{s^{\varrho}Y\{M\sum_{\iota=0}^{\infty} p^{\iota}\upsilon_{\iota}(\xi,\psi) + \sum_{\iota=0}^{\infty} p^{\iota}H_{\iota}(\upsilon_{\iota})\}\right\}\right]. \tag{3.8}$$

Comparison both sides of coefficient p, we get

$$\begin{aligned}
&p^0 : \upsilon_0(\xi,\psi) = F(\xi,\psi),\\
&p^1 : \upsilon_1(\xi,\psi) = Y^{-1}\left[s^{\varrho}Y(M\upsilon_0(\xi,\psi) + H_0(\upsilon))\right],\\
&p^2 : \upsilon_2(\xi,\psi) = Y^{-1}\left[s^{\varrho}Y(M\upsilon_1(\xi,\psi) + H_1(\upsilon))\right],\\
&\vdots\\
&p^{\iota} : \upsilon_{\iota}(\xi,\psi) = Y^{-1}\left[s^{\varrho}Y(M\upsilon_{\iota-1}(\xi,\psi) + H_{\iota-1}(\upsilon))\right], \quad \iota > 0, \iota \in N.
\end{aligned} \tag{3.9}$$

Finally, present the obtained solution and check it with any available analytical or numerical solutions for the given PDE. The $\upsilon_{\iota}(\xi,\psi)$ components can be calculated easily which quickily converges to series form. We can get $p \to 1$,

$$\upsilon(\xi,\psi) = \lim_{M\to\infty}\sum_{\iota=1}^{M} \upsilon_{\iota}(\xi,\psi). \tag{3.10}$$

4. Applications

Problem 4.1. *Consider the space fractional Helmholtz equation*

$$\frac{\partial^{\varrho}\upsilon(\xi,\psi)}{\partial\xi^{\varrho}} + \frac{\partial^2\upsilon(\xi,\psi)}{\partial\psi^2} - \upsilon(\xi,\psi) = 0, \qquad 1 < \varrho \le 2, \tag{4.1}$$

with the ICs

$$\upsilon(0,\psi) = \psi \;\; and \;\; \upsilon_{\xi}(0,\psi) = 0. \tag{4.2}$$

Using the Yang transform of Eq (4.1), we obtained as

$$\frac{1}{s^{\varrho}} Y[\upsilon(\xi,\psi)] = \upsilon(0,\psi)s^{1-\varrho} - Y\left\{\frac{\partial^2\upsilon(\xi,\psi)}{\partial\psi^2} - \upsilon(\xi,\psi)\right\}, \tag{4.3}$$

$$Y[\upsilon(\xi,\psi)] = s\upsilon(0,\psi) - s^{\varrho} Y\left\{\frac{\partial^2\upsilon(\xi,\psi)}{\partial\psi^2} - \upsilon(\xi,\psi)\right\}, \tag{4.4}$$

Taking inverse Yang Transformation, we have

$$Y[\upsilon(\xi,\psi)] = \psi - Y^{-1}\left[s^{\varrho} Y\left\{\frac{\partial^2\upsilon(\xi,\psi)}{\partial\psi^2} - \upsilon(\xi,\psi)\right\}\right], \tag{4.5}$$

Implemented HPM in Eq (4.5), we can achieve as

$$\sum_{\imath=0}^{\infty} p^{\imath}\upsilon_{\imath}(\xi,\psi) = \psi - p\left[Y^{-1}\left\{s^{\varrho} Y\left\{\left(\sum_{\imath=0}^{\infty} p^{\imath}\upsilon_{\imath}(\xi,\psi)\right)_{\psi\psi} - \sum_{\imath=0}^{\infty} p^{\imath}\upsilon_{\imath}(\xi,\psi)\right\}\right\}\right]. \tag{4.6}$$

On both sides comparing coefficients of p, we get

$$\begin{aligned}
&p^0 : \upsilon_0(\xi,\psi) = \psi,\\
&p^1 : \upsilon_1(\xi,\psi) = -Y^{-1}\left[s^{\varrho} Y\left\{\frac{\partial^2\upsilon_0(\xi,\psi)}{\partial\psi^2} - \upsilon_0(\xi,\psi)\right\}\right] = \frac{\xi^{\varrho}}{\Gamma(\varrho+1)}\psi,\\
&p^2 : \upsilon_2(\xi,\psi) = -Y^{-1}\left[s^{\varrho} Y\left\{\frac{\partial^2\upsilon_1(\xi,\psi)}{\partial\psi^2} - \upsilon_1(\xi,\psi)\right\}\right] = \frac{\xi^{2\varrho}}{\Gamma(2\varrho+1)}\psi,\\
&p^3 : \upsilon_3(\xi,\psi) = -Y^{-1}\left[s^{\varrho} Y\left\{\frac{\partial^2\upsilon_2(\xi,\psi)}{\partial\psi^2} - \upsilon_2(\xi,\psi)\right\}\right] = \frac{\xi^{3\varrho}}{\Gamma(3\varrho+1)}\psi,\\
&p^4 : \upsilon_4(\xi,\psi) = -Y^{-1}\left[s^{\varrho} Y\left\{\frac{\partial^2\upsilon_3(\xi,\psi)}{\partial\psi^2} - \upsilon_3(\xi,\psi)\right\}\right] = \frac{\xi^{4\varrho}}{\Gamma(4\varrho+1)}\psi,\\
&\vdots
\end{aligned} \tag{4.7}$$

The series type result of the first problem example is

$$\begin{aligned}
&\upsilon(\xi,\psi) = \upsilon_0(\xi,\psi) + \upsilon_1(\xi,\psi) + \upsilon_2(\xi,\psi) + \upsilon_3(\xi,\psi) + \upsilon_4(\xi,\psi) + \cdots\\
&\upsilon(\xi,\psi) = \psi\left[1 + \frac{\xi^{\varrho}}{\Gamma(\varrho+1)} + \frac{\xi^{2\varrho}}{\Gamma(2\varrho+1)} + \frac{x^{3\varrho}}{\Gamma(3\varrho+1)} + \frac{\xi^{4\varrho}}{\Gamma(4\varrho+1)} + \cdots\right].
\end{aligned} \tag{4.8}$$

The exact solution is

$$\upsilon(\xi,\psi) = \psi\cosh\xi.$$

Similarly y-space can be calculated as:

$$\frac{\partial^{\varrho}\upsilon(\xi,\psi)}{\partial\psi^{\varrho}} + \frac{\partial^2\upsilon(\xi,\psi)}{\partial\xi^2} - \upsilon(\xi,\psi) = 0, \tag{4.9}$$

with the IC

$$\upsilon(\xi, 0) = \xi. \tag{4.10}$$

Thus, the solution of the above Eq (4.9) is obtain as

$$\upsilon(\xi, \psi) = \xi\left(1 + \frac{\psi^{\varrho}}{\Gamma(\varrho+1)} + \frac{\psi^{2\varrho}}{\Gamma(2\varrho+1)} + \frac{\psi^{3\varrho}}{\Gamma(3\varrho+1)} + \frac{\psi^{4\varrho}}{\Gamma(4\varrho+1)} + \ldots\right),$$

in the case when $\varrho = 2$, then the solution through HPTM is

$$\upsilon(\xi, \psi) = \xi \cosh \psi. \tag{4.11}$$

Figure 1 illustrates the exact and HPTM solutions in two-dimensional plots for various values of ϱ ranging from 2 to 1.5, with ξ values ranging from 0 to 1 and ψ set to 1. The solutions are presented in Figure 1a and b for the exact and HPTM methods, respectively. Figure 2 displays the 3-dimensional plots of the exact and HPTM solutions for $\varrho = 2$ and analyzes the point of intersection between the two solutions. Figure 2c and d depict the HPTM solutions at $\varrho = 1.8$ and 1.6 respectively for Problem 4.1. The fractional results were also evaluated for their convergence towards an integer-order result for each problem. Similarly, the figures for the ψ-space can also be generated using the same approach.

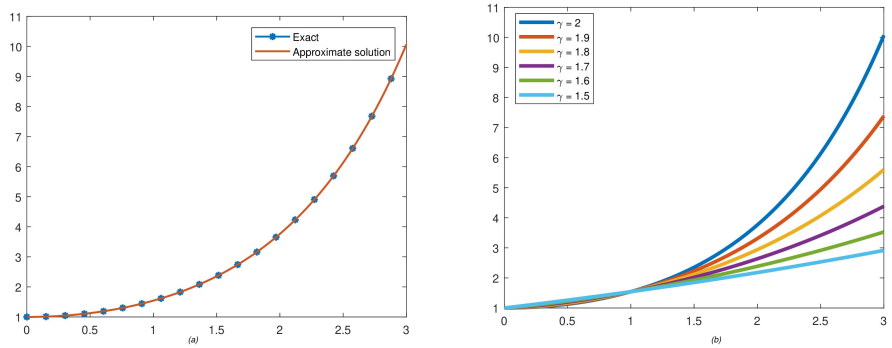

Figure 1. The first graph show that the exact and approximate solution and second HPTM solution at the different fractional-order graph of Problem 4.1.

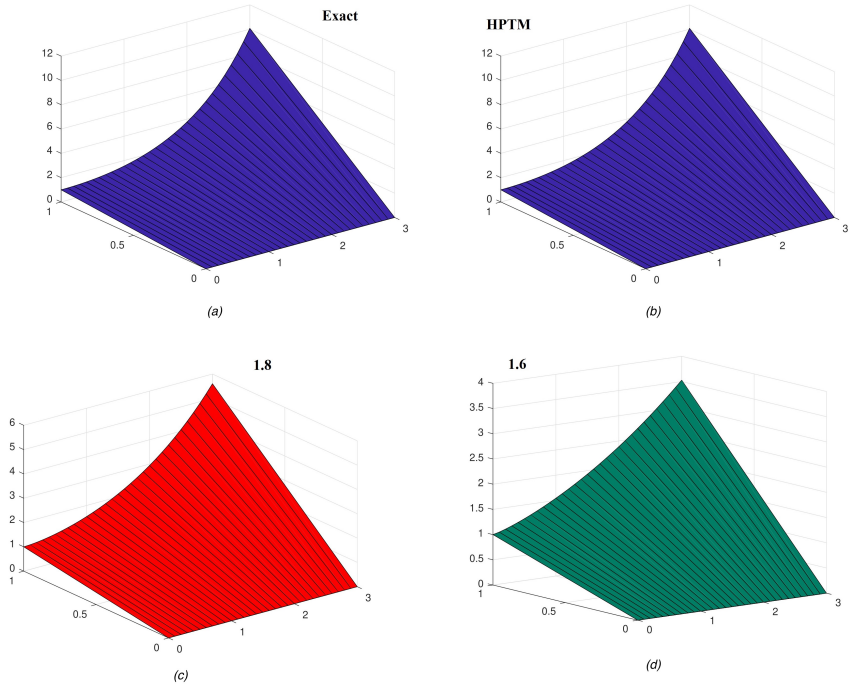

Figure 2. Exact and proposed method solution at various fractional orders of Problem 4.1.

Table 1. Exact and proposed method solution of Problem 4.1 at various fractional orders.

(ξ,ψ)	$\upsilon(\xi,\psi)$ at ϱ =1.5	$\upsilon(\xi,\psi)$ at ϱ =1.75	$(HPTM)$ at $\varrho = 2$	Exact result
(0.2,0.1)	0.2102371	0.2100072	0.2100000	0.2100000
(0.4,0.1)	0.4104630	0.4100141	0.4100000	0.4100000
(0.6,0.1)	0.6106889	0.6100209	0.6100000	0.6100000
(0.2,0.2)	0.2103355	0.2100121	0.2100000	0.2100000
(0.4,0.2)	0.4106550	0.4100237	0.4100000	0.4100000
(0.6,0.2)	0.6109746	0.6100353	0.6100000	0.6100000
(0.2,0.3)	0.2104110	0.2100164	0.2100000	0.2100000
(0.4,0.3)	0.4108025	0.4100321	0.4100000	0.4100000
(0.6,0.3)	0.6111940	0.6100478	0.6100000	0.6100000
(0.2,0.4)	0.2104747	0.2100204	0.2100000	0.2100000
(0.4,0.4)	0.4109269	0.4100399	0.4100000	0.4100000
(0.6,0.4)	0.6113790	0.6100593	0.6100000	0.6100000
(0.2,0.5)	0.2105309	0.2100241	0.2100000	0.2100000
(0.4,0.5)	0.4110365	0.4100471	0.4100000	0.4100000
(0.6,0.5)	0.6115421	0.6100701	0.6100000	0.6100000

Problem 4.2. *Consider the space-fractional HE*

$$\frac{\partial^{\varrho}\upsilon(\xi,\psi)}{\partial\xi^{\varrho}}+\frac{\partial^{2}\upsilon(\xi,\psi)}{\partial\psi^{2}}+5\upsilon(\xi,\psi)=0,\qquad 1<\varrho\leq 2, \tag{4.12}$$

with the ICs

$$\upsilon(0,\psi)=\psi\ \ and\quad \upsilon_{\xi}(0,\psi)=0. \tag{4.13}$$

Using the Yang transform of Eq (4.12), we obtain as

$$\frac{1}{s^{\varrho}}Y[\upsilon(\xi,\psi)]=\upsilon(0,\psi)s^{1-\varrho}-Y\left\{\frac{\partial^{2}\upsilon(\xi,\psi)}{\partial\psi^{2}}+5\upsilon(\xi,\psi)\right\}, \tag{4.14}$$

$$Y[\upsilon(\xi,\psi)]=s\upsilon(0,\psi)-s^{\varrho}Y\left\{\frac{\partial^{2}\upsilon(\xi,\psi)}{\partial\psi^{2}}+5\upsilon(\xi,\psi)\right\}. \tag{4.15}$$

Applying the inverse Yang Transform, we get

$$Y[\upsilon(\xi,\psi)]=\psi-Y^{-1}\left[s^{\varrho}Y\left\{\frac{\partial^{2}\upsilon(\xi,\psi)}{\partial\psi^{2}}+5\upsilon(\xi,\psi)\right\}\right], \tag{4.16}$$

Using the HPM in Eq (4.16), we obtained as

$$\sum_{\iota=0}^{\infty}p^{\iota}\upsilon_{\iota}(\xi,\psi)=\psi-p\left[Y^{-1}\left\{s^{\varrho}Y\left\{\left(\sum_{\iota=0}^{\infty}p^{\iota}\upsilon_{\iota}(\xi,\psi)\right)_{\psi\psi}+5\sum_{\iota=0}^{\infty}p^{\iota}\upsilon_{\iota}(\xi,\psi)\right\}\right\}\right]. \tag{4.17}$$

On both sides comparing coefficients of p, we get

$$\begin{aligned}
&p^{0}:\upsilon_{0}(\xi,\psi)=\psi,\\
&p^{1}:\upsilon_{1}(\xi,\psi)=-Y^{-1}\left[s^{\varrho}Y\left\{\frac{\partial^{2}\upsilon_{0}(\xi,\psi)}{\partial\psi^{2}}+5\upsilon_{0}(\xi,\psi)\right\}\right]=-5\psi\frac{\xi^{\varrho}}{\Gamma(\varrho+1)},\\
&p^{2}:\upsilon_{2}(\xi,\psi)=-Y^{-1}\left[s^{\varrho}Y\left\{\frac{\partial^{2}\upsilon_{1}(\xi,\psi)}{\partial\psi^{2}}+5\upsilon_{1}(\xi,\psi)\right\}\right]=25\psi\frac{\xi^{2\varrho}}{\Gamma(2\varrho+1)},\\
&p^{3}:\upsilon_{3}(\xi,\psi)=-Y^{-1}\left[s^{\varrho}Y\left\{\frac{\partial^{2}\upsilon_{2}(\xi,\psi)}{\partial\psi^{2}}+5\upsilon_{2}(\xi,\psi)\right\}\right]=-125\frac{\xi^{3\varrho}}{\Gamma(3\varrho+1)},\\
&p^{4}:\upsilon_{4}(\xi,\psi)=-Y^{-1}\left[s^{\varrho}Y\left\{\frac{\partial^{2}\upsilon_{3}(\xi,\psi)}{\partial\psi^{2}}+5\upsilon_{3}(\xi,\psi)\right\}\right]=625\psi\frac{\xi^{4\varrho}}{\Gamma(4\varrho+1)},\\
&\vdots
\end{aligned} \tag{4.18}$$

The series type result of second problem as

$$\begin{aligned}
&\upsilon(\xi,\psi)=\upsilon_{0}(\xi,\psi)+\upsilon_{1}(\xi,\psi)+\upsilon_{2}(\xi,\psi)+\upsilon_{3}(\xi,\psi)+\upsilon_{4}(\xi,\psi)+\cdots\\
&\upsilon(\xi,\psi)=\psi\left[1-\frac{5\xi^{\varrho}}{\Gamma(\varrho+1)}+\frac{25\xi^{2\varrho}}{\Gamma(2\varrho+1)}-\frac{125x^{3\varrho}}{\Gamma(3\varrho+1)}+\frac{625\xi^{4\varrho}}{\Gamma(4\varrho+1)}+\cdots\right].
\end{aligned} \tag{4.19}$$

The exact solution is

$$\upsilon(\xi,\psi)=\psi\cos\sqrt{5}\xi.$$

Now similarly, the result of y-space can be calculated with the help of homotopy perturbation

$$\frac{\partial^{\varrho}\upsilon(\xi,\psi)}{\partial\psi^{\varrho}}+\frac{\partial^{2}\upsilon(\xi,\psi)}{\partial\xi^{2}}+5\upsilon(\xi,\psi)=0, \tag{4.20}$$

with the IC

$$\upsilon(\xi,0)=\xi. \tag{4.21}$$

The solution of the Eq (4.20) is expressed as

$$\upsilon(\xi,\psi)=\xi\left(1-\frac{5\psi^{\varrho}}{\Gamma(\varrho+1)}+\frac{25\psi^{2\varrho}}{\Gamma(2\varrho+1)}-\frac{125\psi^{3\varrho}}{\Gamma(3\varrho+1)}+\frac{625\psi^{4\varrho}}{\Gamma(4\varrho+1)}+\cdots\right).$$

The exact solution is

$$\upsilon(\xi,\psi)=\xi\cos\sqrt{5}\psi. \tag{4.22}$$

Figure 3 illustrates the solutions of exact and HPTM in two-dimensional plots, as shown in Figure 3a and b for different values of ϱ, ranging from 2 to 1.5, respectively. The interval considered for ξ is [0, 1], while ψ is constant at 1. The results obtained from the fractional-order model converge to the integer-order solution of the problem. In Figure 4, the 3-dimensional plots of exact and HPTM solutions are presented in Figures (a) and (b), respectively, for $\varrho = 2$. The closed contact of the two solutions is analyzed. Additionally, Figure 4c and d depict the HPTM solutions at $\varrho = 1.8$ and 1.6, respectively, for Problem 4.2. Similarly, graphs for ψ-space can also be generated.

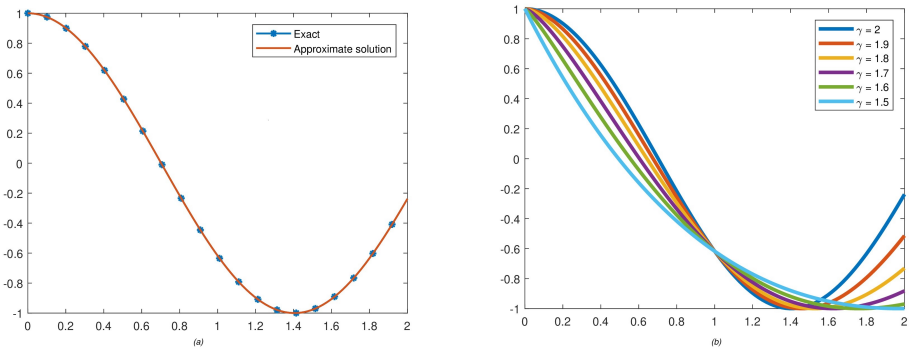

Figure 3. Exact and proposed method solution at various fractional orders of Problem 4.2.

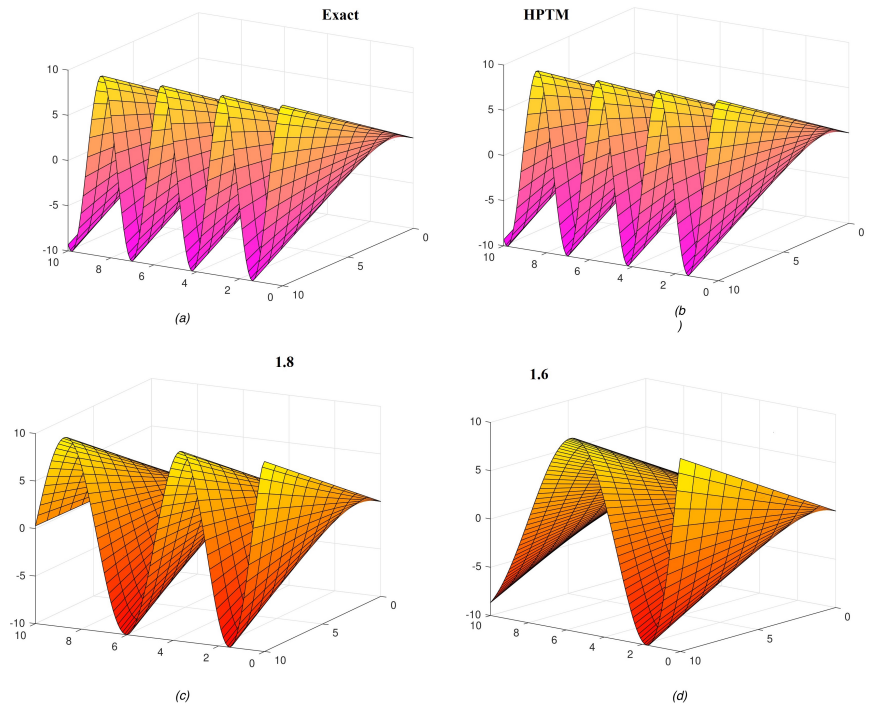

Figure 4. Exact and proposed method solution at various fractional orders of Problem 4.2.

Problem 4.3. *Consider the space-fractional HE*

$$\frac{\partial^{\varrho}\upsilon(\xi,\psi)}{\partial\xi^{\varrho}}+\frac{\partial^{2}\upsilon(\xi,\psi)}{\partial\psi^{2}}-2\upsilon(\xi,\psi)=(12\xi^{2}-3\xi^{4})\sin\psi,\quad 1<\varrho\leq 2,\quad 0\leq\psi\leq 2\pi, \tag{4.23}$$

with the ICs

$$\upsilon(0,\psi)=0\ \ and\quad \upsilon_{\xi}(0,\psi)=0. \tag{4.24}$$

Applying the Yang transform of Eq (4.23), we achieve

$$\frac{1}{s^{\varrho}}Y[\upsilon(\xi,\psi)]=\upsilon(0,\psi)s^{1-\varrho}-Y\left\{\frac{\partial^{2}\upsilon(\xi,\psi)}{\partial\psi^{2}}-2\upsilon(\xi,\psi)\right\}, \tag{4.25}$$

$$Y[\upsilon(\xi,\psi)]=s\upsilon(0,\psi)-s^{\varrho}Y\left\{\frac{\partial^{2}\upsilon(\xi,\psi)}{\partial\psi^{2}}-2\upsilon(\xi,\psi)\right\}. \tag{4.26}$$

Implementing inverse Yang transform, we get

$$Y[\upsilon(\xi,\psi)]=\left(\xi^{4}-\frac{\xi^{6}}{10}\right)\sin\psi-Y^{-1}\left[s^{\varrho}Y\left\{\frac{\partial^{2}\upsilon(\xi,\psi)}{\partial\psi^{2}}-2\upsilon(\xi,\psi)\right\}\right]. \tag{4.27}$$

Applying Homotopy perturbation method in Eq (4.27), we achieved as

$$\sum_{\iota=0}^{\infty}p^{\iota}\upsilon_{\iota}(\xi,\psi)=\psi-p\left[Y^{-1}\left\{s^{\varrho}Y\left\{\left(\sum_{\iota=0}^{\infty}p^{\iota}\upsilon_{\iota}(\xi,\psi)\right)_{\psi\psi}-2\sum_{\iota=0}^{\infty}p^{\iota}\upsilon_{\iota}(\xi,\psi)\right\}\right\}\right]. \tag{4.28}$$

Both sides on comparison coefficients of p, we obtain

$$\begin{aligned}
p^0 &: \upsilon_0(\xi,\psi) = \left(\xi^4 - \frac{\xi^6}{10}\right)\sin\psi,\\
p^1 &: \upsilon_1(\xi,\psi) = -Y^{-1}\left[s^{\varrho}Y\left\{\frac{\partial^2\upsilon_0(\xi,\psi)}{\partial\psi^2} - 2\upsilon_0(\xi,\psi)\right\}\right] = 3\left(\frac{\xi^{\varrho+4}}{\Gamma(\varrho+5)} - \frac{72\xi^{\varrho+6}}{\Gamma(\varrho+7)}\right)\sin\psi,\\
p^2 &: \upsilon_2(\xi,\psi) = -Y^{-1}\left[s^{\varrho}Y\left\{\frac{\partial^2\upsilon_1(\xi,\psi)}{\partial\psi^2} - 2\upsilon_1(\xi,\psi)\right\}\right] = 3\left(\frac{\xi^{2\varrho+4}}{\Gamma(2\varrho+5)} - \frac{216\xi^{2\varrho+6}}{\Gamma(2\varrho+7)}\right)\sin\psi,\\
p^3 &: \upsilon_3(\xi,\psi) = -Y^{-1}\left[s^{\varrho}Y\left\{\frac{\partial^2\upsilon_2(\xi,\psi)}{\partial\psi^2} - 2\upsilon_2(\xi,\psi)\right\}\right] = 3\left(\frac{\xi^{3\varrho+4}}{\Gamma(3\varrho+5)} - \frac{648\xi^{3\varrho+6}}{\Gamma(3\varrho+7)}\right)\sin\psi,\\
p^4 &: \upsilon_4(\xi,\psi) = -Y^{-1}\left[s^{\varrho}Y\left\{\frac{\partial^2\upsilon_3(\xi,\psi)}{\partial\psi^2} - 2\upsilon_3(\xi,\psi)\right\}\right] = 3\left(\frac{\xi^{4\varrho+4}}{\Gamma(4\varrho+5)} - \frac{1944\xi^{2\varrho+6}}{\Gamma(2\varrho+7)}\right)\sin\psi,\\
&\vdots
\end{aligned} \tag{4.29}$$

The series type result of the third problem is

$$\begin{aligned}
\upsilon(\xi,\psi) =& \upsilon_0(\xi,\psi) + \upsilon_1(\xi,\psi) + \upsilon_2(\xi,\psi) + \upsilon_3(\xi,\psi) + \upsilon_4(\xi,\psi) + \cdots\\
\upsilon(\xi,\psi) =& \left(\xi^4 - \frac{\xi^6}{10}\right)\sin\psi + 3\left(\frac{\xi^{\varrho+4}}{\Gamma(\varrho+5)} - \frac{72\xi^{\varrho+6}}{\Gamma(\varrho+7)}\right)\sin\psi + 3\left(\frac{\xi^{2\varrho+4}}{\Gamma(2\varrho+5)} - \frac{216\xi^{2\varrho+6}}{\Gamma(2\varrho+7)}\right)\sin\psi\\
&+ 3\left(\frac{\xi^{3\gamma+4}}{\Gamma(3\varrho+5)} - \frac{648\xi^{3\varrho+6}}{\Gamma(3\varrho+7)}\right)\sin\psi + 3\left(\frac{\xi^{4\varrho+4}}{\Gamma(4\varrho+5)} - \frac{1944\xi^{2\varrho+6}}{\Gamma(2\varrho+7)}\right)\sin\psi + \cdots.
\end{aligned} \tag{4.30}$$

The exact solution is

$$\upsilon(\xi,\psi) = \xi^4\sin\psi.$$

Figure 5a and b display the exact and HPTM solutions, respectively, in a 3-dimensional plot at $\varrho = 2$. *The closed contact between the exact and HPTM solutions is examined. Figure 6 depicts the exact and HPTM solutions in two-dimensional plot for various values of* $\varrho = 2, 1.9, 1.8, 1.7, 1.6, 1.5$ *for* $\xi \in [0,1]$ *and* $\psi = 1$. *The fractional results are observed to approach an integer-order solution of the problem. Similarly, the graphs for* ψ*-space fractional-order derivative can also be plotted.*

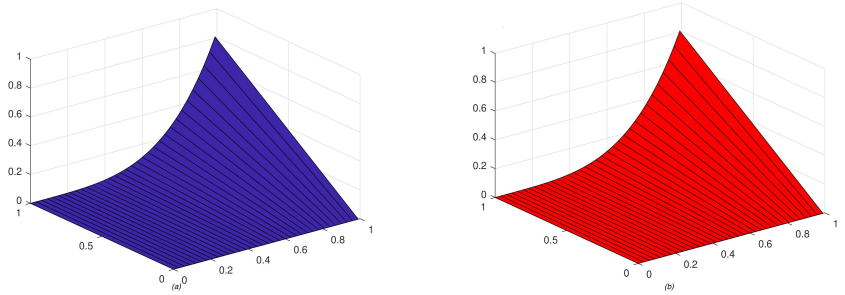

Figure 5. Exact and proposed method solution at various fractional orders of Problem 4.3.

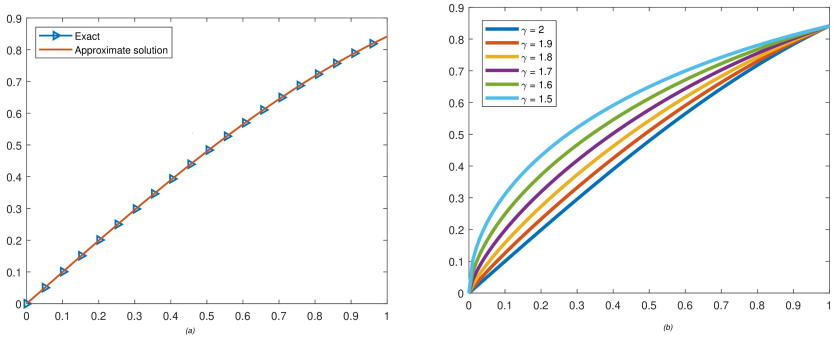

Figure 6. Exact and proposed method solution at various fractional orders of Problem 4.3.

5. Conclusions

In this study, fractional-order Helmholtz equations were solved using the Homotopy Perturbation Yang transform method. Due to the great agreement between the generated approximative solution and the precise solution, the homotopy perturbation Yang transform method was demonstrated to be a successful method for solving partial differential equations with Caputo operators. The computation size of the approach was compared to those required by other numerical methods to demonstrate how tiny it is. Additionally, the procedure's quick convergence demonstrates its dependability and marks a notable advancement in the way linear and non-linear fractional-order partial differential equations are solved.

Acknowledgements

This research has been funded by Deputy for Research & Innovation, Ministry of Education through Initiative of Institutional Funding at University of Ha'il–Saudi Arabia through project number IFP-22 064.

Conflict of interest

The authors declare that they have no competing interests.

References

1. J. Li, X. N. Su, K. Y. Zhao, Barycentric interpolation collocation algorithm to solve fractional differential equations, *Math. Comput. Simulat.*, **205** (2023), 340–367. https://doi.org/10.1016/j.matcom.2022.10.005
2. M. M. Al-Sawalha, R. P. Agarwal, R. Shah, O. Y. Ababneh, W. Weera, A reliable way to deal with fractional-order equations that describe the unsteady flow of a polytropic gas, *Mathematics*, **10** (2022), 2293. https://doi.org/10.3390/math10132293

3. L. A. Said, A. H. Madian, A. G. Radwan, A. M. Soliman, Fractional order oscillator with independent control of phase and frequency, In *2014 2nd International Conference on Electronic Design (ICED)*, 2014, 224–229. https://doi.org/10.1109/ICED.2014.7015803
4. J. T. Machado, V. Kiryakova, F. Mainardi, Recent history of fractional calculus, *Commun. Nonlinear Sci. Numer. Simul.*, **16** (2011), 1140–1153. https://doi.org/10.1016/j.cnsns.2010.05.027
5. J. Sabatier, O. P. Agrawal, J. A. Tenreiro Machado, *Advances in Fractional Calculus*, Dordrecht: Springer, 2007.
6. D. Baleanu, K. Diethelm, E. Scalas, J. J. Trujillo, *Fractional Calculus: Models and Numerical Methods*, World Scientific, 2012. https://doi.org/10.1142/10044
7. L. Debnath, Recent applications of fractional calculus to science and engineering, *Int. J. Math. Math. Sci.*, **2003** (2003), 1–30. https://doi.org/10.1155/S0161171203301486
8. M. M. Al-Sawalha, A. S. Alshehry, K. Nonlaopon, R. Shah, O. Y. Ababneh, Fractional view analysis of delay differential equations via numerical method, *AIMS Mathematics*, **7** (2022), 20510–20523. https://doi.org/10.3934/math.20221123
9. S. Mukhtar, R. Shah, S. Noor, The numerical investigation of a fractional-order multi-dimensional model of Navier-Stokes equation via novel techniques, *Symmetry*, **14** (2022), 1102. https://doi.org/10.3390/sym14061102
10. M. M. Al-Sawalha, A. S. Alshehry, K. Nonlaopon, R. Shah, O. Y. Ababneh, Approximate analytical solution of time-fractional vibration equation via reliable numerical algorithm, *AIMS Mathematics*, **7** (2022), 19739–19757. https://doi.org/10.3934/math.20221082
11. M. M. Al-Sawalha, R. Shah, A. Khan, O. Y. Ababneh, T. Botmart, Fractional view analysis of Kersten-Krasil'shchik coupled KdV-mKdV systems with non-singular kernel derivatives, *AIMS Mathematics*, **7** (2022), 18334–18359. https://doi.org/10.3934/math.20221010
12. Y. Kai, S. Q. Chen, K. Zhang, Z. X. Yin, Exact solutions and dynamic properties of a nonlinear fourth-order time-fractional partial differential equation, *Wave. Random Complex*, 2022. https://doi.org/10.1080/17455030.2022.2044541
13. F. Ihlenburg, I. Babuska, Finite element solution of the Helmholtz equation with high wave number part II: The h-p version of the FEM, *SIAM J. Numer. Anal.*, **34** (1997), 315–358. https://doi.org/10.1137/S0036142994272337
14. S. M. El-Sayed, D. Kaya, Comparing numerical methods for Helmholtz equation model problem, *Appl. Math. Comput.*, **150** (2004), 763–773. https://doi.org/10.1016/S0096-3003(03)00305-9
15. Y. K. Cheung, W. G. Jin, O. C. Zienkiewicz, Solution of Helmholtz equation by Trefftz method, *Int. J. Numer. Meth. Eng.*, **32** (1991), 63–78. https://doi.org/10.1002/nme.1620320105
16. A. Prakash, M. Goyal, S. Gupta, Numerical simulation of space-fractional Helmholtz equation arising in seismic wave propagation, imaging and inversion, *Pramana*, **93** (2019), 28. http://doi.org/10.1007/s12043-019-1773-8
17. S. Nguyen, C. Delcarte, A spectral collocation method to solve Helmholtz problems with boundary conditions involving mixed tangential and normal derivatives, *J. Comput. Phys.*, **200** (2004), 34–49. https://doi.org/10.1016/j.jcp.2004.03.004

18. X. Li, Z. Q. Dong, L. P. Wang, X. D. Niu, H. Yamaguchi, D. C. Li, et al., A magnetic field coupling fractional step lattice Boltzmann model for the complex interfacial behavior in magnetic multiphase flows, *Appl. Math. Model.*, **117** (2023), 219–250. https://doi.org/10.1016/j.apm.2022.12.025
19. X. L. Xie, T. F. Wang, W. Zhang, Existence of solutions for the (p,q)-Laplacian equation with nonlocal Choquard reaction, *Appl. Math. Lett.*, **135** (2023), 108418. https://doi.org/10.1016/j.aml.2022.108418
20. L. Wang, H. Zhao, X. Liu, Z. L. Zhang, X. H. Xia, S. Evans, Optimal remanufacturing service resource allocation for generalized growth of retired mechanical products: Maximizing matching efficiency, *IEEE Access*, **9** (2021), 89655–89674. https://doi.org/10.1109/ACCESS.2021.3089896
21. S. Abuasad, K. Moaddy, I. Hashim, Analytical treatment of two-dimensional fractional Helmholtz equations, *J. King Saud Univ. Sci.*, **31** (2019), 659–666. https://doi.org/10.1016/j.jksus.2018.02.002
22. X. Wang, X. J. Lyu, Experimental study on vertical water entry of twin spheres side-by-side, *Ocean Eng.*, **221** (2021), 108508. https://doi.org/10.1016/j.oceaneng.2020.108508
23. Y. Hu, J. X. Qing, Z. H. Liu, Z. J. Conrad, J. N. Cao, X. P. Zhang, Hovering efficiency optimization of the ducted propeller with weight penalty taken into account, *Aerosp. Sci. Technol.*, **117** (2021), 106937. https://doi.org/10.1016/j.ast.2021.106937
24. H. Y. Jin, Z. A. Wang, Global stabilization of the full attraction-repulsion Keller-Segel system, *Discrete Contin. Dyn. Syst.*, **40** (2020), 3509–3527. https://doi.org/10.3934/dcds.2020027
25. H. Y. Jin, Z. A. Wang, Boundedness, blowup and critical mass phenomenon in competing chemotaxis, *J. Differ. Equ.*, **260** (2016), 162–196. https://doi.org/10.1016/j.jde.2015.08.040
26. H. Y. Jin, Z. A. Wang, Asymptotic dynamics of the one-dimensional attraction-repulsion Keller-Segel model, *Math. Meth. Appl. Sci.*, **38** (2015), 444–457. https://doi.org/10.1002/mma.3080
27. L. Liu, S. Zhang, L. Ch. Zhang, G. Pan, J. Z. Yu, Multi-UUV maneuvering counter-game for dynamic target scenario based on fractional-order recurrent neural network, *IEEE Trans. Cybernetics*, 2022, 1–14. https://doi.org/10.1109/TCYB.2022.3225106
28. N. Iqbal, M. T. Chughtai, R. Ullah, Fractional study of the non-linear Burgers' equations via a semi-analytical technique, *Fractal Fract.*, **7** (2023), 103. https://doi.org/10.3390/fractalfract7020103
29. P. Liu, J. P. Shi, Z. A. Wang, Pattern formation of the attraction-repulsion Keller-Segel system, *Discrete Contin. Dyn. Syst. Ser. B*, **18** (2013), 2597–2625. https://doi.org/10.3934/dcdsb.2013.18.2597
30. M. Alesemi, N. Iqbal, N. Wyal, Novel evaluation of fuzzy fractional Helmholtz equations, *J. Funct. Spaces*, **2022** (2022), 8165019. https://doi.org/10.1155/2022/8165019
31. P. K. Gupta, A. Yildirim, K. N. Rai, Application of He's homotopy perturbation method for multi-dimensional fractional Helmholtz equation, *Internat. J. Numer. Methods Heat Fluid Flow*, **22** (2012), 424–435. https://doi.org/10.1108/09615531211215738

AIMS Press